FLYING QUALITIES ANALYSIS OF A THREE SURFACES AIRCRAFT MODEL

D.P. Coiro, F. Nicolosi, A. De Marco, N. Genito
University of Naples "Federico II", Dipartimento di Progettazione Aeronautica (DPA)
Faculty of Engineering, Via Claudio 21 – 80125 Naples, Italy. Email: coiro@unina.it

Keywords: *Flight Tests, Flight Simulations, Canard, 3LSC*

Abstract

Since twenty years ago canard configurations have become more and more usual, especially for light and very light aircraft. Positive features of canard configurations not always comply to the control and stability requirements for all c.g. range and for every flight condition, unless an artificial stability augmenter system is installed. In three lifting surfaces configurations (3LSC) a small horizontal surface behind the wing is added to compensate the reduction of the aircraft stability due to the canard. 3LSC give flexibility in selecting the aircraft geometry for what concerns the payload/wing/fuselage relative position. 3LSC also reduce the total lifting area, with consequent reduction of total wetted area and aerodynamic drag.

Design of a three lifting surfaces radio-controlled model has been carried out at Dipartimento di Progettazione Aeronautica (DPA) by the authors in the last year. This prototype has been designed to test the influence of the canard on the aircraft aerodynamics, static and dynamic stability and flying qualities at high angles of attack. The model can fly with and without canard and for this reason the areas of the lifting surfaces are not optimized. This model is equipped with several sensors to measure all flight parameters and surface deflections. Problems related to the data acquisition and recording, and innovative solutions for the measurement of angle of attack and of sideslip are presented in this paper.

The paper also deals with the analysis of numerically predicted flight characteristics of the present prototype, and their use for virtual flight simulations. Simulated maneuvers presented in this paper provide useful information about canard influence on the aircraft flight qualities and estimation of all aerodynamic characteristics. Flight tests are planned in these days while writing this paper.

1 Introduction

In the last twenty years canard configurations have become more and more usual, especially for light and very light aircrafts. After the Wrights' first flying machines, the revival of canard configuration on classical "backward-built" airplanes has been pushed by experimental aircrafts and by the evolution of the numerical and experimental tools necessary to accomplish the design of this type of configuration. Some aircrafts, such as Burt Rutan's famous designs like VariEZ and LongEZ, Boomerang and Defiant, have contributed with their commercial success to the popularity of canard configurations. A canard configuration is characterized by positive features (i.e., reduced wing area and aircraft drag), but cannot always comply to the control and stability requirements for all c.g. ranges and for every flight condition, unless an artificial stability augmenter system is installed. But this would be a difficult task for small aircraft.

Some authors [1, 2] have shown through detailed analysis advantages and disadvantages of canard configuration on classical aft-tailed ones. The best compromise is to add a small horizontal surface behind the wing to compensate the reduction of the aircraft stability due to the presence of the canard surface, and so to adopt a three lifting surfaces configuration (3LSC).

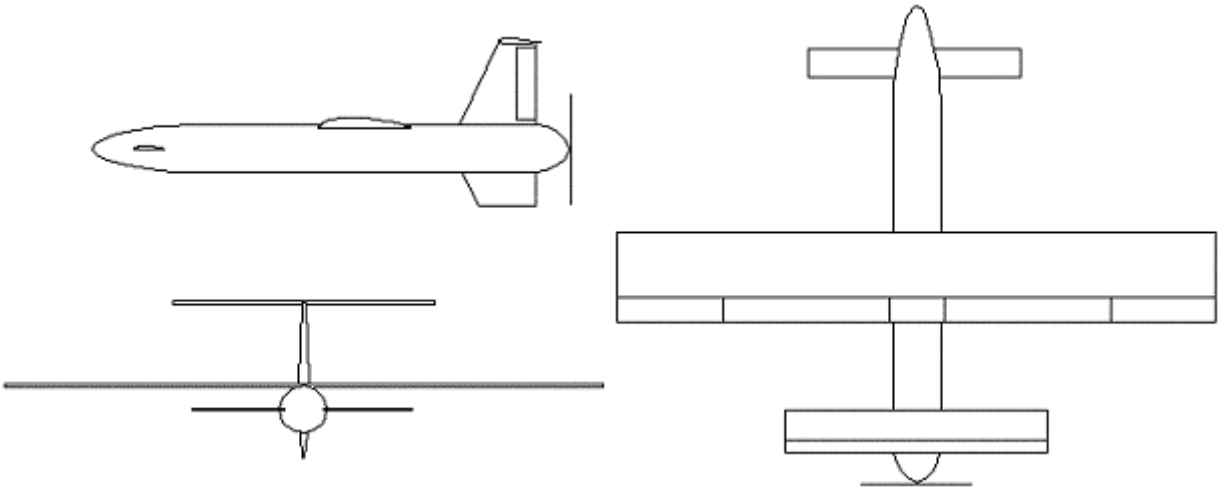

Fig. 1. The 3-view sketch of the model.

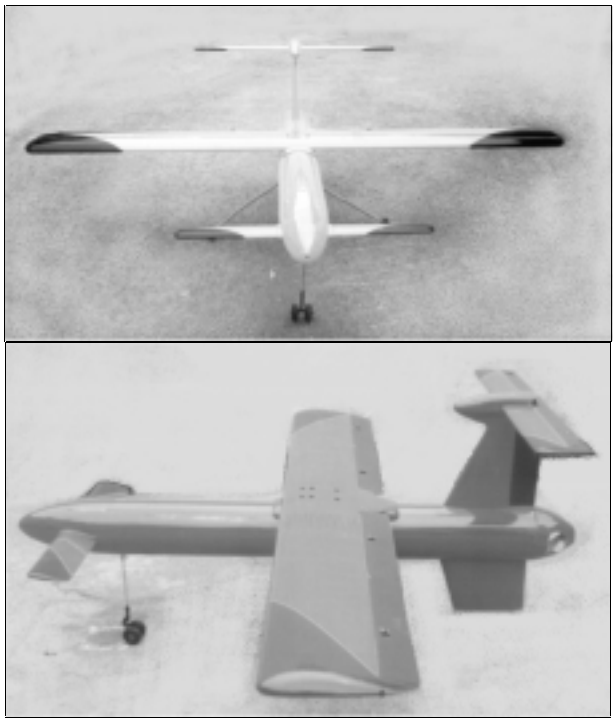

Fig. 2. Views of the prototype.

One of the major advantages of the 3LSC derives from the added flexibility in selecting the aircraft geometry for what concerns the payload/wing/fuselage relative position, due to the possibility of complying with control & stability requirements for a larger range of c.g. positions. Some authors [3] have written papers on theoretical minimum induced drag of 3LS airplanes in trim. Another significant advantage of 3LSC is the reduction of the total lifting area required to fly, with consequent reduction of total wetted area and aerodynamic drag. Smrcek et al. [4] and Ostowari et al [5] have investigated, through numerical and wind-tunnel tests, the effect of canard and its position on global aerodynamic coefficients.

In recent years there is a growing interest in the innovative 3LSC. It has been adopted in the design of some light and commuter aircraft (Eagle 150, Molniya-1, Etruria E-180) and for the well known Piaggio P180 (the only modern transport aircraft with the 3LSC).

The design of a 3LS radio-controlled model has been carried out at Dipartimento di Progettazione Aeronautica (DPA) by the authors in the last year. The model is intended to be a UAV prototype, and its construction has been completed in 2002. A 3-view of the model is shown in fig. 1, and two photographs are shown in fig. 2. Tab. 1 reports main dimensions and weights. The maximum take-off weight is about 15 *kg* with a pay-load of about 4 *kg* and about 1 *l* of fuel.

This R/C model has been designed mainly to test the influence of the canard surface on aircraft aerodynamic characteristics, static and dynamic stability, and flying qualities also at high angles of attack. To this purpose the model

can fly with and without canard, and so the areas of the lifting surfaces are not optimized. Through the shift of the payload and fuel it will be possible to modify the c.g. position between 5% and 30% of the wing chord to fly with the same static stability margin (SSM) with and without canard.

A very important solid motivation for the project is that the model should be a low-cost flying testing platform for all sensors and acquisition/measurement systems (for both flight parameter analysis and external monitoring, i.e., climatic and ground control).

As final but not negligible advantage, the small aircraft can be an easy, low-cost system for teaching purposes (in particular useful for flight dynamics and flight maneuver reproduction and analysis).

The model has been built in glass-fiber composite material with a wooden fuselage frame and wing ribs to reduce the empty weight and to have a clean and well finished wetted surface. The fuselage shape and the lifting surfaces planform (see again fig. 1) have been chosen in order to have very simple and economical constructive solutions. The fuselage sections have a circular shape and have been molded through a cheap 0.2 *m* diameter PVC tube. The engine and the pushing propeller have been put in the fuselage rear part to have an undisturbed flow for canard and wing surfaces. The propeller effectiveness (behind the fuselage) has been tested in DPA wind-tunnel to verify that the necessary thrust is guaranteed.

The wing and canard airfoils have been chosen to have high lift at low flight Reynolds numbers together with a contained viscous drag and a reasonable pitching moment. The wing has been designed with effective ailerons (to ensure lateral control at low speed) and with flap, although the equilibrated maximum lift with full flap (1.96) is not so high as the lift without a flap (1.68) due to the strong increment in pitching moment that the tail is not able to compensate with reasonable elevator deflections. The predicted stall speed with flap is about 40 *km/h* and without flap about 44 *km/h*, so the model should not have any take-off and landing problem.

Due to the short distance between c.g. and the vertical tail a second vertical fin has been added below the fuselage to ensure good directional stability. This is also necessary to protect the rear propeller from contact with the ground. The design has been accomplished using a code named *AEREO* [6], which has been developed in recent years at DPA to predict all aerodynamic characteristics in linear and non-linear conditions (high angles of attack) and all flight performances as well as flying qualities of propeller driven aircraft, and has recently been extended to deal with canard and 3LSC.

Tab. 1. Main dimensions and weights of the 3LS model.

Dimensions	
wing area	0.95 m^2
wing span	2.50 *m*
wing chord	0.38 *m*
canard span	0.90 *m*
canard chord	0.14 *m*
canard area	0.13 m^2
fuselage length	2.00 *m*
fuselage diam.	0.20 *m*
horiz. tail area.	0.20 m^2
horiz. tail chord (movable part 44% of chord)	0.18 *m*
tot vert. tail area	0.13 m^2
Weights	
Empty structural weight	8.30 *kg*
Payload and fuel weight	4.50 *kg*
Engine (3.5 *hp*) weight	1.80 *kg*
Max TO weight (WTO)	14.6 *kg*

2 Configuration and Structural Design

The main goal of this aircraft is to allow flight parameter measurement and estimation of canard influence (especially at high angles of attack) on aircraft aerodynamics and flight characteristics. Ref. [7] contains a detailed discussion of the design criteria adopted for this prototype.

To have a pay-load of about 4 *kg*, and to ensure a good and easy disposition of the instrumentation, a fuselage diameter of about 0.20 *m* was chosen. The consequent useful load is around 5 *kg*. The estimated structural weight

was around 8 *kg*. A good working distance for canard and horizontal tail and a fuselage fineness ratio higher than 8, to ensure good propeller efficiency, leads to a 2 *m* total length fuselage. The estimated fuselage weight is around 2 and 3 *kg*. Assuming a weight of about 5 *kg* for wing, tailplanes and canard, an empty structural weight between 8 and 9 *kg* is expected. With the engine total weight around 2 *kg* the maximum take-off weight is around 15 *kg*.

Stall speed requirements, assuming a maximum lift coefficient around 1.7 in clean condition and around 2.0 in full-flap condition, a maximum wing load of about 15 kg/m^2 can easily be evaluated. This gives a wing surface of about 1 m^2.

The 4 stroke - 2 cylinder engine chosen, the *OS-Gemini*, delivers a maximum power of about 4 *hp* at 7000 *rpm*. With 0.50 *m* diameter a propeller, the expected practical working condition is around 7000 *rpm*.

An imposed maximum climb rate at *S*/L of 3.5 *m/s* leads (see [7]) to a necessary wing span *b* of about 2.5 *m*. It also seems reasonable to have a wing span higher than the canard span.

The horizontal tailplane dimensions should give good stability and control power to fly with and without canard. A movable part (equilibrator) extended over 44% of the total horizontal plane chord ensures a good longitudinal control.

The final configuration corresponds to the one shown in fig. 1, with all main dimensions reported in tab. 1. The configuration has the following relevant features:

a) The simple fuselage shape allows a low-cost molding. The fuselage skin structure in glass-fiber with some added carbon-fiber was simply molded with a 0.20 *m* PVC tube. Some carbon stringers were added to increase longitudinal stiffness. The fuselage is thus characterized by two high quality wood main spar frames allowing wing and undercarriage connections.

b) The wing, canard and tailplane structures are made by wooden ribs numerically controlled machine milled and with a mixed glass-carbon fiber composite skin.

c) A thickness of about 2 *mm* was chosen for almost all model surfaces. The chosen structure ensures a very good safety margin without leading to excessive weight. Considering the experimental task and a possible future fully automatic flight, this design philosophy seems reasonable and efficient.

d) The weight of the complete structure with exact dimensions and thickness was then estimated and are reported in ref. [7] together with weights obtained after construction. The maximum take-off weight WTO, adding engine weight and useful load is then 14.6 *kg*. WTO of model without canard is 14.2 *kg*.

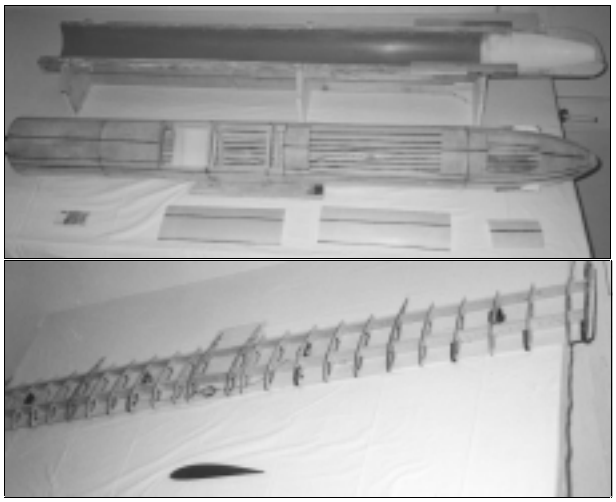

Fig. 3. Fuselage (up), wing internal structure and airfoil (down) in construction.

e) In terms of aircraft c.g. position the main goal will be to guarantee a longitudinal static stability margin (SSM) in cruise condition of about 10% for configurations both with and without canard, taking into account that the neutral point can be estimated to be around 15% of the chord with canard and 40% without, the useful load has been located in the fuselage forward part at 23 *cm* from the nose with canard and 44 *cm* without. *The full weight c.g. position is imposed to be around 5% of wing chord with canard and 29% without.* For the wing and canard the high-lift low-Reynolds number airfoil SD7062 was chosen (see ref. [8]). The fuselage in construction and wing internal structure before molding are shown in fig. 3.

3 Aerodynamic analysis

3.1 AEREO code and extension to canard and 3LS configuration

The *AEREO* code has been developed by the authors in recent years to predict all aerodynamic characteristics in linear and non-linear conditions of propeller driven aircraft.

The code is based on longitudinal [9] and lateral-directional [10] semi-empirical methods, like those proposed by J. Roskam [11] mixed with more sophisticated calculations, such as wing lift and drag predictions up to stall. The code also predicts all performances, static and dynamic stability characteristics, and is similar to the well known *AAA* software [12]. The code was originally written to deal with the classical aft-tailed configuration, especially for light aircraft and sailplanes [6]. The code has recently been expanded and improved to deal with canard or 3LSC. With the simple horse-shoe vortex theory the calculation of mutual influence of wing and canard has been implemented. Maturing experiences and tools integration [13] has been one of the main goals of the author´s activity at DPA in recent years, and the aerodynamic and flight behavior analysis of this configuration certainly goes in that direction.

The authors also have good experience of wind-tunnel tests for analysis and optimization of light aircrafts [14] and of integration and comparison of numerical calculations with experimental results [15].

3.2 Results – lift, drag and moment coefficient

Mutual induction of canard on wing (downwash angle ε_W) and wing on canard (upwash angle ε_C) have been estimated in *AEREO* code through a simple horse-shoe vortex theory and a global value is obtained through average along the span (see details in ref. [16]).

Fig. 4 show contributions of wing, wing-body, canard and horizontal tail versus α (with respect to the fuselage center line) to lift and moment coefficients. It can be observed that canard stalls around α=16° and this reflects on global lift and especially the global moment coefficient curve. An equilibrated lift curve has been obtained for the configuration with and without canard, and for the configuration with canard with 30° flap deflected. The results are shown in fig. 5.

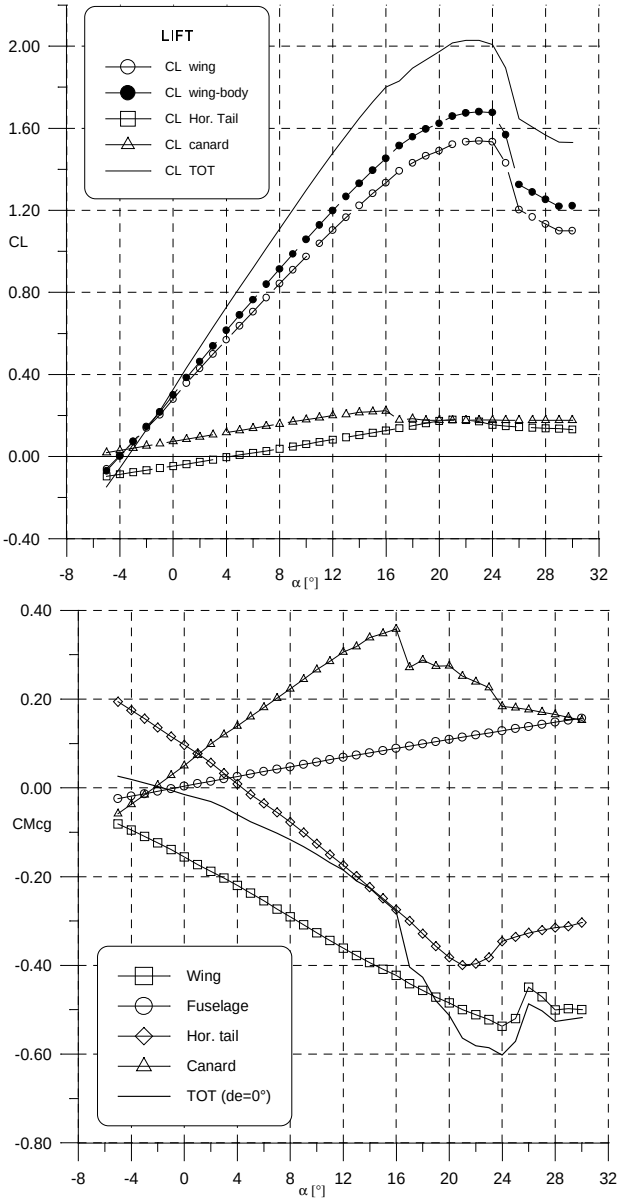

Fig. 4. Contributions to the lift and moment coefficients; c.g. pos. 5% *c*, and δ_e=0°.

A maximum equilibrated lift coefficient of 1.66 is obtained for the 3LSC (and c.g. at 5% of *c*), a value of 1.61 for the configuration without canard and a value of 1.97 for the 30° flapped 3LSC. The resulting stall speeds for the 3LSC are about 40 *km/h* and 44 *km/h*, respectively, for the clean and flapped conditions.

From the equilibrated (trimmed) drag polar for the configuration with and without canard, fig. 6, it can be observed that, at high speeds, the 3LSC leads to a higher drag than the configuration without canard, but lower drag (lower global induced drag) at low speeds. The global Oswald efficiency factor "*e*" for the 3LSC in trimmed conditions is about 0.85, showing a good value for an aircraft that should operate at low speed.

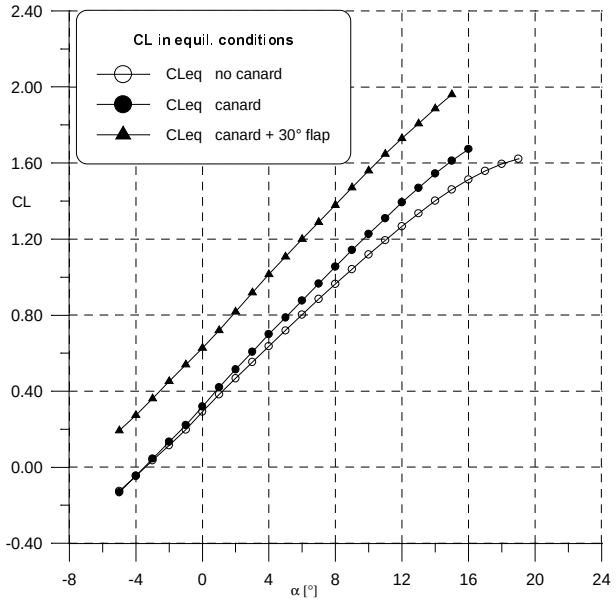

Fig. 5. Equilibrated lift coefficient.

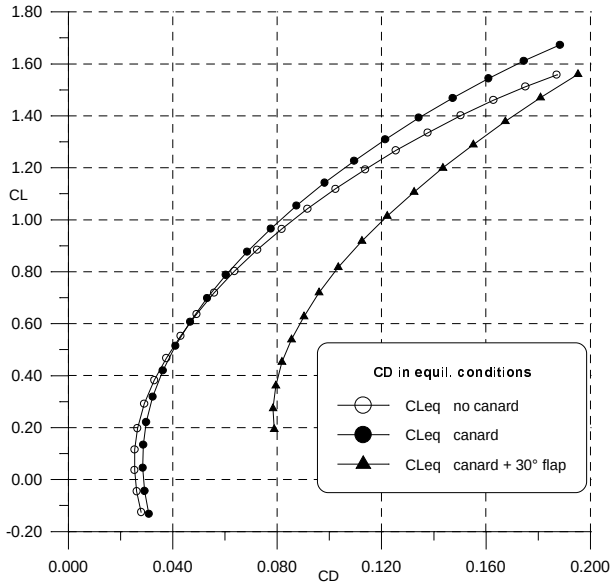

Fig. 6. Trimmed Drag polar.

The required deflections at stall are always acceptable (–15° for the clean configuration, and –22° for the flapped one). See ref. [16] for details.

3.3 Results – Neutral point - Static and dynamic stability

The neutral point versus trimmed lift coefficient for configuration with and without canard are shown in fig. 7. The SSM is about 13% at cruise conditions (C_L=0.50) for both configurations. High stability at low speed can be recognized.

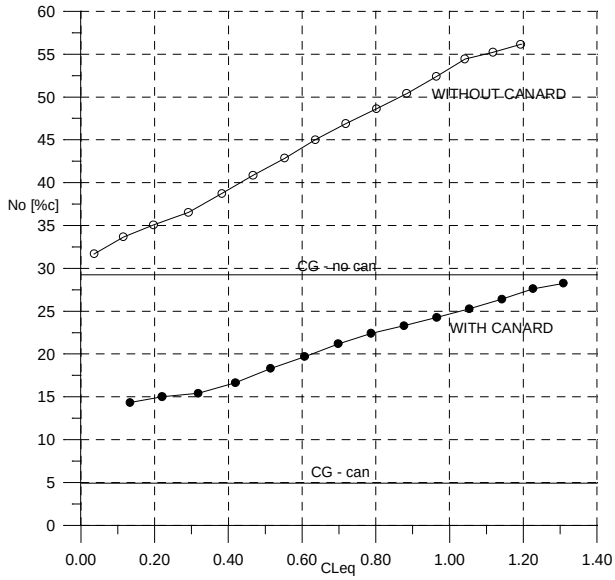

Fig. 7. Neutral stability point.

Tab. 2. Static stability derivatives.

	w canard	w/o canard
Long.		
$C_{L\alpha}$	5.60 [1/rad]	5.20 [1/rad]
$C_{M\alpha}$	−0.48 [1/rad]	−0.59 [1/rad]
$C_{M\alpha'}$	−1.94	−1.18
C_{Mq}	−8.02	−4.41
Lat.-dir.		
C_{lb}	−0.059 [1/rad]	−0.064 [1/rad]
C_{lp}	-0.52	−0.51
C_{nb}	0.090 [1/rad]	0.079 [1/rad]

Longitudinal and lateral-directional stability derivatives have been evaluated for configuration with canard and without canard. Tab. 2 shows the most significant stability derivatives at cruise conditions for configuration with and without canard (α' is dα/dt). Note that the 3LSC leads to a higher lift curve slope and higher aerodynamic damping (unsteady $C_{M\alpha'}$ and C_{Mq} derivatives). Tab. 3 shows the dynamic

stability characteristics. Long and short period characteristics show that the 3LSC leads to a slightly lower frequency for long period motion and a higher frequency for short period motion. The damping is always higher with the canard.

Table 3. Dynamic longitudinal stability.

	w canard	**w/o canard**
Short Period		
Freq. [Hz]	0.710	0.66
Damping	0.817	0.70
Long Period		
Freq. [Hz]	0.070	0.087
Damping	0.026	−0.016

4 Performances and wind tunnel tests on engine and propeller

To verify the behavior of the engine coupled to different pushing propellers, the model fuselage with rear mounted engine was set up in the wind tunnel as shown in fig. 8. Drag, lift and moment were measured with an internal 3-component strain gage balance, and recorded with the use of an A/D acquisition system.

Necessary and available power curves at S/L for configurations with and without canard were evaluated with two possible propellers: 18/6 (D=0.46 *m*, blade angle β_{75} =8°) and 18/10 (D=0.46 *m*, β_{75} =13.3°). Maximum power of 4.0 *hp* and maximum propeller efficiency 0.50 were assumed (propeller works behind the fuselage).

Unfortunately due to the lack of model aircraft employing pushing propellers, these are available only in certain diameter/pitch combinations. We tried 18/10, 18/6, 15/8, 15/6, 14/6, of which only the last was available in PVC, while the others were all made of wood.

Engine *rpm* was also measured. The tests were performed, for each wind speed, setting three throttle levels and recording *rpm*, forces and moments. Some other angles of attack were also investigated. It can easily be recognized that there were many possible combinations of the free parameters, and while writing this paper we are still analyzing the recorded data.

No significant reduction in propeller efficiency was measured at high angles of attack, indicating that the position of the propeller and the shape of the rear part of fuselage were fine. We also performed some tests turning the model 180° to test the differences between the pushing and tracting propellers, and first analysis of data shows that there is no appreciable difference.

Fig. 8. Fuselage installed in the tunnel.

Tab. 4. Performances at S/L of the engine with propeller 18/10.

	w. canard	**w/o canard**
Max level speed	125 *km/h*	127 *km/h*
Max cruise speed (75% of power)	118 *km/h*	122 *km/h*
Max RC	5.2 *m/s*	5.3 *m/s*
Max cruise range	17 *km*	19 *km*
Max aer. efficiency	12.8	12.9
Take-off run	45 *m*	40 *m*
Landing run	54 *m*	50 *m*

The engine was tested with 18 *in* (0.46 *m* diameter) propellers with two different blade pitch angles, 9° (18/6) and 13° (18/10). Fig. 9 shows the corresponding experimentally measured power curves. The 18/6 propeller does not give a good efficiency (around 0.25), which leads to very low available power. The 18/10 propeller gives good propulsive power with an efficiency around 0.5. In fig. 9 the experimental available power curves are reported along with the numerical relative to necessary power. The measured drag was found to be higher than the predicted drag. The predicted maximum level speed with 18/10 propeller is around 125 *km/h*. Engine performances with the 18/10 propeller

are reported in tab. 4, which shows very good flight and take-off characteristics.

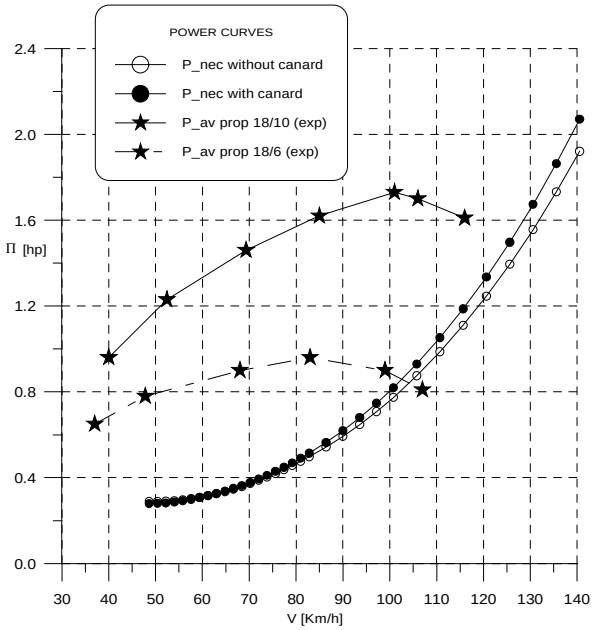

Fig. 9. Required and available power curves, 18/10 and 18/6 prop (exp).

6 The instrumentation for data acquisition

The R/C model will be equipped with the following data acquisition devices: (*i*) an inertial platform, see fig. 10, for the measure of roll and pitch angles, angular rates, and of linear accelerations; (*ii*) a vertical accelerometer for the measure of the load factor; (*iii*) a temperature probe; (*iv*) potentiometers, see fig. 11, for the measure of elevator, ailerons, and rudder deflections; (*v*) pressure probes; (*vi*) a special probe for the measure of angles of attack and sideslip, see fig. 12.

This latter innovative instrument has been completely designed at DPA. It is based on well known *Hall effect* to measure, through the variation of a magnetic field, both angles of attack and sideslip. This simple principle, being implemented through economical electronic components, keeps the price of the probe very low. The probe is also a Pitot tube and it is used to measure the dynamic pressure as well. Test campaign in the wind tunnel is undergoing to calibrate the whole system. The probe is being patented.

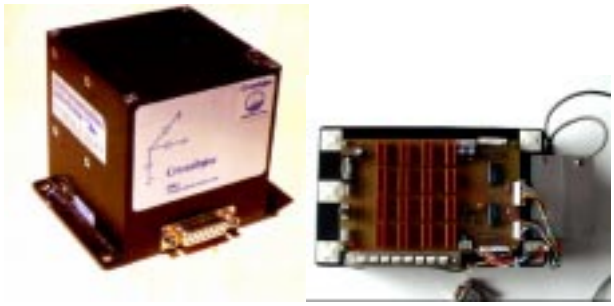

Fig. 10. The inertial platform *CrossBow DMU-6X* (left), and the Data Acquisition System designed by authors (right).

Fig. 11. Potenziometer for the measure of rudder angular deflection, as installed on a *DG400* sailplane.

Fig. 12. Probe for the measure of the angles of attack and of sideslip.

The data acquisition system (DAS) is based on *Tattletale Model* 8 chip by *Onset Company*, extended with *Persistor CF8* equipped with commercially available high storage capability (i.e. 64 *Mb*) *Compact Flash Cards*. The DAS allows the reading of 32 channels, 16 of which can be conditioned according to the user's needs, 8 are dedicated to the *DMU* platform, and the remaining 8 are used by potentiometers.

The DAS has been used in flight tests on a *DG400* sailplane [16]. A numerical code based on *Maximum Likelihood Estimation* was

developed and used to estimate all longitudinal and lateral-directional stability derivatives of the sailplane, analyzing flight recorded data. The same proven procedure will be used for the present model aircraft.

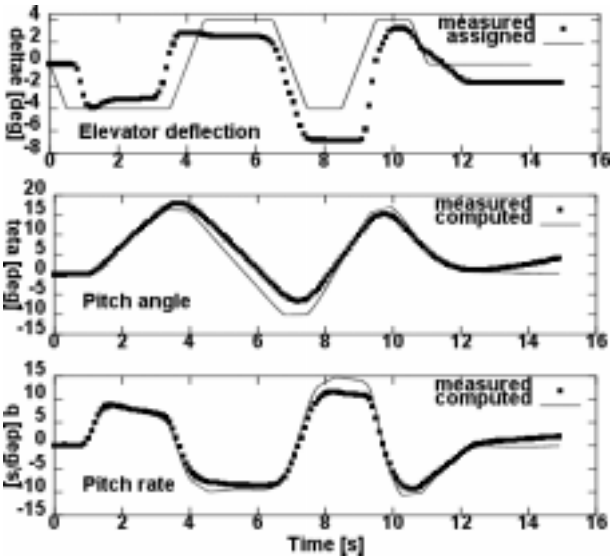

Fig. 13. A data acquisition for the maneuver performed by a *DG400* sailplane.

A maneuver performed on a *DG400* is shown in fig. 13 as elevator deflection, pitch angle, and pitch rate vs. time. Measured and predicted computed data are compared (see ref. [16]).

7 Simulations

At the moment that the paper is being written, flight tests are being performed, and then results will be presented at the congress.

Time histories reported below are numerically obtained by a solver developed by the authors, implementing the 6-dof non-linear equations of motion for a rigid aircraft. Aerodynamic, dynamic, and control coefficients occurring in the equations are those predicted by the *AEREO* code. Here the aim is essentially the prediction and analysis of the 3LS model behaviour as a support for flight tests, since simulations allow the determination of possible uncontrollable evolutions in response to a particular maneuver or initial condition.

Below are showed the forced simulated response of the model to different maneuvers. Initial conditions for the first two examples are: S/L altitude, velocity 25 *m/s*, angle of attack α=0.6°, equilibrator deflection δ_e = –0.76°, thrust 12 N.

The aerodynamic, dynamic, and control coefficients corresponding to the assumed initial conditions, are reported in tab. 5 below, as given by *AEREO* code.

Tab. 5. Parameters predicted by *AEREO* code for the maneuvers reported in figures below.

Coeff.		Coeff.	
$C_{L\alpha}$ [*1/rad*]	5.60	$C_{Y\beta}$ [*1/rad*]	–0.44
$C_{L\dot{\alpha}}$	1.23	$C_{Y\delta r}$ [*1/rad*]	0.17
$C_{m\alpha}$ [*1/rad*]	–0.53	$C_{\ell\beta}$ [*1/rad*]	–0.054
$C_{m\dot{\alpha}}$	–2.12	$C_{\ell p}$	–0.59
C_{Lq}	4.58	$C_{\ell r}$	0.15
C_{mq}	–10.85	$C_{\ell\delta a}$ [*1/rad*]	–0.12
$C_{L\delta e}$ [*1/rad*]	0.88	$C_{\ell\delta r}$ [*1/rad*]	0.014
$C_{m\delta e}$ [*1/rad*]	–1.83	$C_{n\beta}$ [*1/rad*]	0.089
$C_{D\alpha}$ [*1/rad*]	0.17	C_{np}	–0.032
$C_{D\delta e}$ [*1/rad*]	–0.044	C_{nr}	–0.098
		$C_{n\delta a}$ [*1/rad*]	0.0067
		$C_{n\delta r}$ [*1/rad*]	–0.055
		$C_{Y\beta}$ [*1/rad*]	–0.44

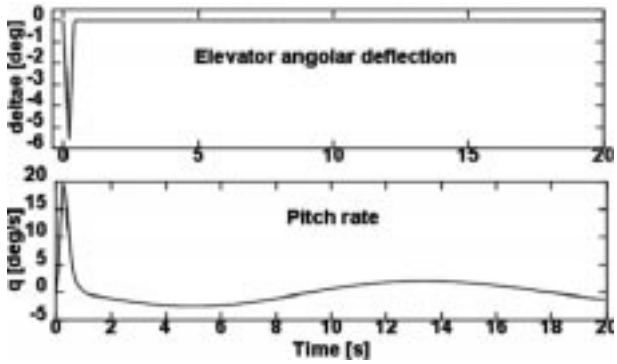

Fig. 14. Simulated elevator maneuver; deflection, δ_e, (top); pitch rate, *q*, vs. time.

Fig. 14 shows the pitch rate time history for the reported impulsive equilibrator maneuver. The quick response and stabilization in visible. Fig. 15 the roll rate time history for reported aileron maneuver. A good aileron effectiveness is clearly observable, as oscillation are damped very quickly. Fig. 16 shows a typical stall manoeuvre. Stall speed is around 43 *km/h*.

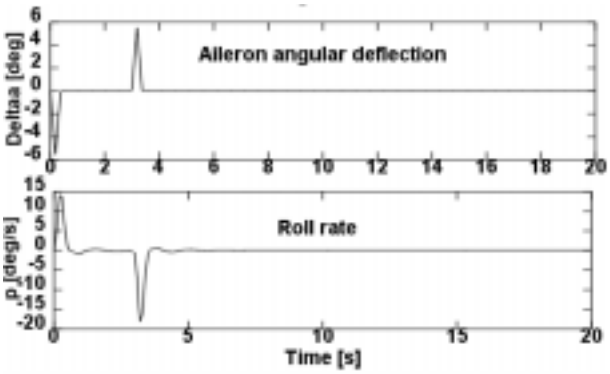

Fig. 15. Simulated aileron maneuver; angular deflection, δ_a, (top); roll rate, *p*, vs. time.

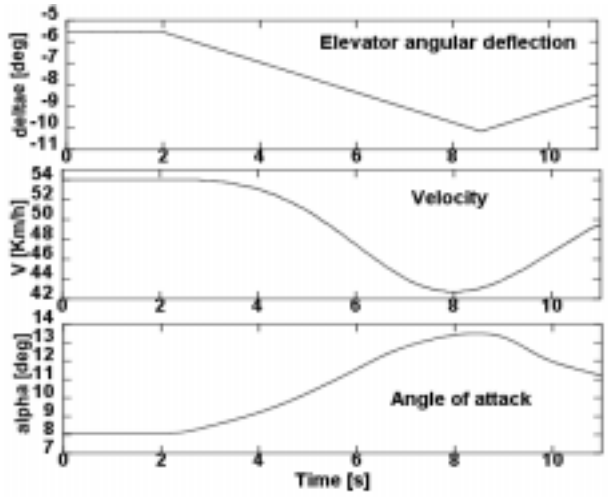

Fig. 16. Simulated stall manouver.

8 Conclusions

Design, aerodynamic and preliminary performance estimation of a 3LS R/C aircraft have been performed. Canard influence on lift, drag and moment coefficients, and on aircraft static and dynamic stability have been carefully evaluated and shown.. Available power curves versus speed have been measured in the wind-tunnel. Body drag has been also measured. Estimated performances are in good agreement with aircraft design and desired flight characteristics, Examples of some flight simulations have been reported. The model is instrumented to measure all flight parameters. Flight tests are being performed at the moment that the paper is being written.

References

[1] McGeer, T., Kroo, I. A Fundamental Comparison of Canard and Conventional Configurations. *Journal of Aircraft*, Vol. 20, November 1983.

[2] Selberg, B.P., Rokhsaz, K. Aerodynamic Tradeoff Study of Conventional, Canard, and Trisurface Aircraft Systems. *Journal of Aircraft*, Vol. 23, October 1986.

[3] Kendall, E. R. The Theoretical Minimum Induced Drag of Three-Surface Airplanes in Trim. *Journal of Aircraft*, Vol. 22, October 1985.

[4] Ostowari, C., Naik, D. Experimental Study of Three-Lifting-Surface Configuration. *Journal of Aircraft*, vol. 25, February 1988.

[5] Patek, Z., Smrcek, L. Aerodynamic characteristics of multi-surface aircraft configurations. *Aircraft Design*, Vol. 2, 1999, pp. 191-206.

[6] Coiro, D. P., Nicolosi, F. Aerodynamics Dynamics and Performance Prediction of Sailplanes and Light Aircraft. *Technical Soaring*, Vol. 24, No. 2, April 2000.

[7] Coiro D. P., Nicolosi F. Design of a three surface R/C aircraft model. *Acta Polytechnica – Journal of Advanced Engineering*. Vol. 42, No. 1, 2002.

[8] Lyon, C.A., Selig, S. et al. Summary of Low-Speed Airfoil Data, vol. 3. *SoarTech Pubblications*, Virginia, 1997, ISBN 0-9646747-3-4, pp. 256-263.

[9] Wolowicz, H. C. and Yancey, B. R.. Longitudinal Aerodynamic Characteristics of Light, Twin-Engine, Propeller-Driven Airplanes. NASA TN D-6800, 1972.

[10] Wolowicz, H. C. and Yancey, B. R. Lateral-Directional Aerodynamic Characteristics of Light, Twin-Engine, Propeller-Driven Airplanes. NASA TN D-6946, 1972.

[11] Roskam, J. *Airplane Design. Part VI : Preliminary Calculation of Aerodynamic, Thrust and Power Characteristic*. Ed. Roskam Aviation 1987

[12] Roskam, J. *AAA, Advanced Aircraft Analysis software*. DAR Corporation, Lawrence, Kansas.

[13] Coiro, D.P., Nicolosi, F. Aircraft Design through Numerical and Experimental Techniques Developed at DPA. *Aircraft Design*, Vol. 4, No. 1 , March, 2001 ISSN 1369-8869.

[14] Giordano, V., Nicolosi, F., Coiro, D.P., Di Leo, L., Design and Aerodynamic Optimization of a New Reconnaissance Very Light Aircraft Through Wind Tunnel Tests, RTA/AVT *Symposium on Aerodynamic Design and Optimization of Flight Vehicles in a Concurrent Multi-disciplinary environment*, Ottawa (CANADA), October 1999.

[15] Giordano, V., Coiro, D.P., Nicolosi, F. Reconnaissance Very Light Aircraft Design. Wind-Tunnel and Numerical Investigation. *Engineering Mechanics*, Vol. 7, No. 2, 2000, pp. 93-107.

[16] Coiro D. P., Nicolosi F., De Marco A. Dynamic Behavior and Performances Determination of DG400 Sailplane through Flight Tests. Accepted by *Technical Soaring Journal*, 2002.